Supporting Information

Kim et al. 10.1073/pnas.1720121115

SI Materials and Methods

Animals. All studies were carried out according to the protocols that were approved by the Institutional Animal Care and Use Committee at Stanford University (APLAC-23785). We used wild-type CBA/CaJ, *Tecta*$^{C1509G/C1509G}$ (1), and *Tyr*-DT-A (2) mice. All mice were 4- to 6-wk old. CBA/CaJ mice have normal auditory thresholds whereas *Tecta*$^{C1509G/C1509G}$ and *Tyr*-DT-A mice have no ABR thresholds to 80-dB SPL stimuli, indicating a severe-to-profound hearing loss. Mice were anesthetized using ketamine (100 mg/kg) and xylazine (10 mg/kg). For some experiments, furosemide (RL-0202; Hospira) was injected intraperitoneally (200 mg/kg) in anesthetized mice immediately before the blast exposure.

Blast Chamber. The blast chamber to deliver blast waves to anesthetized mice was custom-built and has been fully described (3). Compressed air in this system is suddenly released and travels down a 272-cm tube that is 11.5 cm in diameter. This sharpens the profile of the blast wave, increasing the peak pressure and reducing the time duration of the pressure wave. The mouse was suspended such that only the ears receive the full impact of the blast, whereas the body was shielded to prevent systemic trauma. The blast wave profile was recorded for every experiment by a high-speed pressure transducer (PCB Piezotronics) that was positioned just below the mouse. The blast pressure can be controlled based upon the amount of air we compress into the chamber. For these experiments, we used a peak blast pressure of 130 ± 9 kPa (~196-dB SPL).

Noise Exposure. Band-pass–filtered white noise (100-dB SPL, 8–16 kHz) was delivered to mice for 2 h using a well-established protocol (4, 5). Mice were awake in their cage during the noise exposure.

In Vivo OCT Imaging and Vibrometry. Under anesthesia, we surgically opened the left middle ear bulla to access the apical turn of the cochlea without disturbing the otic capsule bone. The design of our OCT system has been previously reported (6). Briefly, our custom-built system comprised a broadband swept-source with a center wavelength of 1,310-nm and 200-kHz sweep rate (MEMS-VCSEL; Thorlabs), 100-nm bandwidth, dual-balanced photodetector (WL-BPD600MA; Wieserlabs), and an 800-MHz digitizer (NI-5772; National Instruments). The power on the sample was 16 mW and the lateral and axial resolutions of the images are 9.8 μm and 15 μm in air, respectively.

Two-dimensional imaging was done by repeatedly scanning the laser to collect cross-sectional images in the x and z dimensions. To quantify endolymph volume (Fig. S7), we collected a volume stack of cross-sectional images, moving the y position in 7.5-μm steps over a 150-μm length of the BM (i.e., 20 cross-sections per mouse). We used Amira 5.4 software (Visage Imaging) to volume-render 3D images. The scala media region was then segmented and the volume measured. The perilymph volume within scala vestibuli was also measured using the same technique. The person measuring the volumes was blinded to the experimental group, although frankly, in most cases it was quite obvious based upon the highly visual nature of endolymphatic hydrops demonstrated by OCT.

To measure BM and TM vibrations, we presented sound stimuli using an earbud headphone calibrated over the desired frequency range of 2–14 kHz and intensity range of 10- to 80-dB SPL. We placed this adjacent to the ear canal and presented 200-ms sound stimuli while measuring the vibrations of the BM and TM using our system, as previously described (6–8). The vibrational noise floor of our system depends upon the signal-to-noise ratio of the structure under study, but was roughly 0.1 nm for these experiments. The gain of cochlear amplification was determined by normalizing the displacement in responses to 10- and 80-dB SPL stimuli and calculating the difference.

Intracochlear Perilymphatic Perfusion. Under anesthesia, we performed a complete exchange of perilymph by removing the stapes from the oval window and inserting a glass micropipette with a 50-μm diameter tip containing artificial perilymph through the round window membrane. A syringe pump (New Era Pump Systems) was connected to provide constant perfusion. For "rapid" perfusion (Figs. 3 and 5 *A–C*), the instillation rate was 50 μL/min over 3 min; for "slow" perfusion (Fig. 6 *M–O*), the instillation rate was 8 μL/min over 1 h. With both approaches, complete exchange of perilymph could be verified by eye based upon the volume of fluid emanating out of the oval window. Hypotonic artificial perilymph (294 mOsm/kg) was composed of 140 mM NaCl, 2 mM KCl, 2 mM $MgCl_2$, 2 mM $CaCl_2$, and 20 mM Hepes. The osmolality of the perilymph was increased as desired by adding additional Hepes to create normotonic (304 mOsm/kg) and hypertonic (314 mOsm/kg) perilymph. For some experiments, we added 100 μM CNQX disodium salt (1045; TOCRIS) to the artificial perilymph. For all solutions, the pH was adjusted to 7.4 and the osmolality was verified using a freezing pressure osmometer (Advanced Instruments).

For some experiments, gold nanoparticles (50 nm diameter, 753645; Sigma-Aldrich) were suspended in the artificial perilymph. To do this, we centrifuged the vial that the nanoparticles come in and removed the PBS supernatant. We then added 1 mL of artificial perilymph, and suspended the nanoparticles by vigorous pipetting. Cross-sectional OCT images of the cochlea were then collected before and after the nanoparticle perfusion. Offline, the average pixel intensities of discrete regions within scala vestibuli and scala media were measured. The percent change in pixel intensity was calculated by normalizing the change in pixel intensity to the pixel intensity before perfusion.

Application of Solutions to the Round Window Membrane. Under anesthesia, we applied solutions of different osmolalities to the extracochlear surface of the round window membrane. Under anesthesia, we either surgically opened the middle ear bulla, as described above, or simply filled up the middle ear space through the blast-induced tympanic membrane perforation. Normotonic saline (304 mOsm/kg) was composed of 150 mM NaCl and 20 mM Hepes. Hypertonic saline (1,504 mOsm/kg) was composed of 800 mM NaCl and 20 mM Hepes. Normotonic artificial perilymph (304 mOsm/kg) was composed of 140 mM NaCl, 4 mM KCl, 2 mM $MgCl_2$, 2 mM $CaCl_2$, 10 mM Hepes, and 10 mM glucose. Hypertonic artificial perilymph (1,532 mOsm/kg) was created by adding 990 mM glucose to the normotonic artificial perilymph. Hypotonic saline or artificial perilymph was simply distilled water (0 mOsm/kg). Other solutions tested included glycerol (~3,500 mOsm/kg) or 0.9% saline with glucose added to create (1,434 mOsm/kg). For all solutions, the pH was adjusted to 7.4 and the osmolality was verified using a freezing pressure osmometer (Advanced Instruments).

Blinded, Randomized, Prospective Study Methodology. The normotonic and hypertonic test solutions were prepared ahead of time. The two test solutions looked identical, and the vials were coded

so that the investigators performing the experiment were blinded throughout. The person who prepared the test solutions was not involved in any other part of this trial, and the coding record was kept in a private, locked drawer so that nobody involved with the mice, the ABR/DPOAE measurements, the histology, or counting of synapses had access.

Thirty minutes after blast exposure, 100 μL of test solution was instilled into the ears. This was simplified by the fact that all mice had blast-induced traumatic perforations in the tympanic membrane. Therefore, we simply filled up the middle ears and external ear canals with a pipette and no surgery was performed. Only the left ears were treated. For the next 5.5 h, the mice were maintained under anesthesia, lying left side up to keep the test solution in contact with the round window membrane. Additional test solution was instilled as needed to keep the ear canals full during this time. Then, the mice were awakened and returned to their cages.

ABR and DPOAE thresholds were measured before the blast, 1 d, 7 d, 1 mo, and 2 mo after the blast. After 2 mo, the mice were killed, both cochleae were harvested, and immunolabeling was performed to count hair cells and synaptic ribbons. The coded data were put into an Excel spreadsheet. In a public laboratory meeting where the senior author (J.S.O.), the experimenters, the person who prepared the solutions, and all other research personnel in the laboratory were present, the code was then broken and we averaged the data for the mice in each of the two treated cohorts. The right untreated (but still blast-exposed) ear of the experimental mice and age-matched, unexposed control mice formed two additional cohorts.

Histological Preparations. Cochleae were fixed in 4% paraformaldehyde (EMS) at room temperature for 1 h. For decalcification, they were immersed in 0.5 M EDTA (AMRESCO) for 6 h at room temperature, and then washed three times in 1× PBS (Fisher Scientific). For whole-mount preparations of the cochlear epithelium, we dissected the organs of Corti from the cochleae under a stereo microscope. The cochlear epithelium was divided into three parts: apex, middle, and base and laid flat on a glass slide. For the TUNEL assay of spiral ganglion neurons, fixed and decalcified whole cochleae were embedded in OCT compound (Tissue-Tek). The cochleae were sectioned into 20-μm slices using a cryotome before performing the TUNEL assay.

Immunohistochemistry. Dissected cochlear tissues were blocked with 5% donkey serum, 0.1% Triton-X 100, 1% BSA, and 0.02% sodium azide (NaN_3) in PBS at pH 7.4 for 1 h at room temperature. We applied primary antibodies which were diluted in the same blocking solution, and stored them overnight at 4 °C. For CtBP2 primary antibody, we stored it two overnight at 4 °C and 2 h at 37 °C. After three times washing in PBST (0.1% Triton-X 100 in 1× PBS), the tissues were incubated with secondary antibodies diluted in 0.1% Triton-X 100, 0.1% BSA and 0.02% NaN_3 in PBS for 1 h at room temperature. After washing them three times in 1× PBS, the tissues were mounted on glass slides using Dako Fluorescent Mounting Medium (Dako North America), and allowed to set overnight in the dark at 4 °C before confocal imaging.

We used primary antibodies against the following markers: myosin VIIa (hair cell marker; 1:200; 25–6790; *Proteus* BioSciences), Prestin (OHC marker; 1:200; sc-22692; Santa Cruz Biotechnology), Tuj1 (neural class III β-tubulin marker; 1:200; MAB5564; EMD Millipore), CtBP2 (synaptic ribbon marker; 1:200; sc-5967; Santa Cruz Biotechnology), and Homer (post synaptic density protein marker, 1:800; 160003; Synaptic Systems). The secondary antibodies were conjugated with Alexa Fluor 488, 546, and 647 (1:500; A11055, A10040, and A31571; Life Technologies). In some preparations, Alexa Fluor 488-conjugated phalloidin labeling (F-actin; 1:200; A12379; Invitrogen) was performed with secondary antibody treatment (1 h at room temperature). The TUNEL assay was achieved using ApopTag plus fluorescein in situ apoptosis detection kit [S7111; EMD Millipore as recommended. We used Prolong Gold antifade reagent with DAPI (P36931; Invitrogen)] for mounting the tissue with the TUNEL assay.

Immunostained cochlear tissues were imaged with a LSM700 confocal microscope (Zeiss) to generate *z*-stacks. We counted the number of hair cells, presynaptic ribbons, and postsynaptic densities using ImageJ software (National Institutes of Health). Accurately counting ribbon synapses is a labor-intensive process (Fig. S8). This was done by selected only the fluorescence color of interest, scrolling through the *z*-stack images one by one, and counting the synaptic densities under each IHC and OHC. We only counted those densities that were present on at least two sequential images. The rate of presynaptic to postsynaptic puncta colocalization was calculated by dividing the number of overlapping puncta (defined as those that had yellow between the green and red labels) by the total number of Homer puncta.

Scanning Electron Imaging. Inner ears from the mice were dissected in fixative (2.5% glutaraldehyde; 4% formaldehyde; 0.05 mM Hepes buffer pH 7.2; 10 mM $CaCl_2$; 5 mM $MgCl_2$; 0.9% NaCl). A hole was poked at the apex of the cochlea and fixative was flushed trough the round window. The samples were fixed first for 2 h at room temperature in this fixative, then in 1% Osmium Tetroxide in washing buffer (0.05 mM Hepes Buffer pH 7.2; 10 mM $CaCl_2$; 5 mM $MgCl_2$; 0.9% NaCl) for 1.5 h, and then rinsed extensively in washing buffer. The samples were dissected in the washing buffer to remove the stria vascularis, Reissner's membrane, and TM. The samples were refixed in 1% Osmium Tetroxide in washing buffer for 1 h then rinsed extensively again. Finally, the samples were dehydrated and processed to critical drying point (Autosamdri-815A; Tousimis). The cochleae were mounted on a stud with silver paint and sputter coated with 5 nm of iridium (EMS150T S; Electron Microscopy Sciences). Samples were imaged at 5 kV with a FEI Magellan 400 XHR Field Emission Scanning Electron Microscope at the Stanford Nano Shared Facilities.

ABR and DPOAE Measurements. ABR potentials were measured with a bioamplifier (DP-311, Warner Instruments) using three needle electrodes positioned in the ventral surface of the tympanic bulla, the vertex of the skull, and the hind leg (9). The stimulus was a 5-ms sine wave tone pip of alternating polarity with $\cos^2$ envelope rise and fall times of 0.5 ms and a repetition time of 41.5 ms. The range of stimulus intensity was from 10- to 80-dB SPL (10-dB steps) and that of frequency was from 4 to 80 kHz. However, the maximum stimulus intensity that could be delivered by our sound system varied with the frequency. Some frequencies had a maximum stimulus intensity of only 70-dB SPL. We averaged 260 responses at each stimulus intensity. The peak-to-peak value of the ABR waveform was measured at each frequency, and the threshold was determined to be when the ABR was 5 SDs above the noise floor. We set the threshold to be 80-dB SPL when the ABR was not detected at 80-dB SPL for averaging purpose.

DPOAEs were measured by a probe tip microphone in the external auditory canal (9). We used the sound stimuli, two sine wave tones of differing frequencies (F2 = 1.2 × F1, F2: 4 ~ 46 kHz), for eliciting DPOAEs. The two tones were from 20- to 80-dB SPL (10-dB steps). The amplitude of the distortion product (2 × F1 − F2) was determined by fast Fourier transform. The threshold was calculated to be when the DPOAE was >5-dB SPL and 2 SDs above the noise floor. We set the threshold to be 80-dB SPL when the DPOAE was not detected at 80-dB SPL for averaging purpose.

Statistical Analysis. Statistical analyses were performed using Excel (Microsoft) and Origin (OriginLab). For three or more groups,

we first performed an ANOVA analysis. For a P value < 0.05, we then followed up using t tests to compare pairs of subgroups. We compared data between groups using the unpaired, two-tailed Student's t test. We compared repeated measures within the same group using the paired, two-tailed Student's t test. P < 0.05 were considered statistically significant. To compare ABR and DPOAE thresholds, we performed multiple linear regression controlling for frequency. All error bars are the SEM. All statistical tests not specifically provided in the text are listed in Table S1.

1. Xia A, et al. (2010) Deficient forward transduction and enhanced reverse transduction in the alpha tectorin C1509G human hearing loss mutation. *Dis Model Mech* 3:209–223.
2. Kim HJ, et al. (2013) Precise toxigenic ablation of intermediate cells abolishes the "battery" of the cochlear duct. *J Neurosci* 33:14601–14606.
3. Cho S-IIS-I, et al. (2013) Mechanisms of hearing loss after blast injury to the ear. *PLoS One* 8:e67618.
4. Liu CCC, et al. (2011) Biophysical mechanisms underlying outer hair cell loss associated with a shortened tectorial membrane. *J Assoc Res Otolaryngol* 12:577–594.
5. Kujawa SG, Liberman MC (2009) Adding insult to injury: Cochlear nerve degeneration after "temporary" noise-induced hearing loss. *J Neurosci* 29:14077–14085.
6. Lee HY, et al. (2015) Noninvasive in vivo imaging reveals differences between tectorial membrane and basilar membrane traveling waves in the mouse cochlea. *Proc Natl Acad Sci USA* 112:3128–3133.
7. Gao SS, et al. (2014) Vibration of the organ of Corti within the cochlear apex in mice. *J Neurophysiol* 112:1192–1204.
8. Gao SS, et al. (2013) In vivo vibrometry inside the apex of the mouse cochlea using spectral domain optical coherence tomography. *Biomed Opt Express* 4:230–240.
9. Xia A, et al. (2007) Altered traveling wave propagation and reduced endocochlear potential associated with cochlear dysplasia in the BETA2/NeuroD1 null mouse. *J Assoc Res Otolaryngol* 8:447–463.

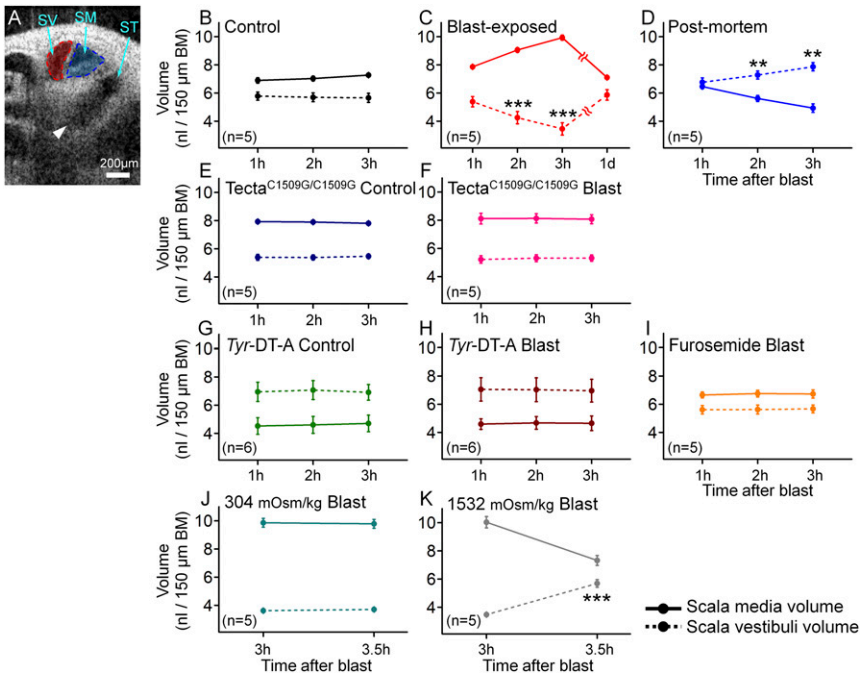

Fig. S1. Changes in perilymph volume within scala vestibuli are opposite the changes in endolymph volume within scala media. (*A*) Cross-sectional OCT image of the mouse cochlea. The red highlights of the region of scala vestibuli and the blue highlights of the region of scala media manually segmented out to calculate perilymph and endolymph volumes, respectively. Scala tympani volume could not be reliably measured because its deep boundary was usually not clear enough (white arrowhead). Scala vestibuli and scala media volumes in living control mice (*B*), blast-exposed mice (*C*), unexposed control mice postmortem (*D*), unexposed *Tecta*$^{C1509G/C1509G}$ control mice (*E*), blast-exposed *Tecta*$^{C1509G/C1509G}$ mice (*F*), unexposed *Tyr*-DT-A control mice (*G*), blast-exposed *Tyr*-DT-A mice (*H*), blast-exposed furosemide-treated mice (*I*), blast-exposed normotonic perilymph-treated mice (*J*), and blast-exposed hypertonic perilymph-treated mice (*K*). $^{**}P < 0.01$, $^{***}P < 0.001$.

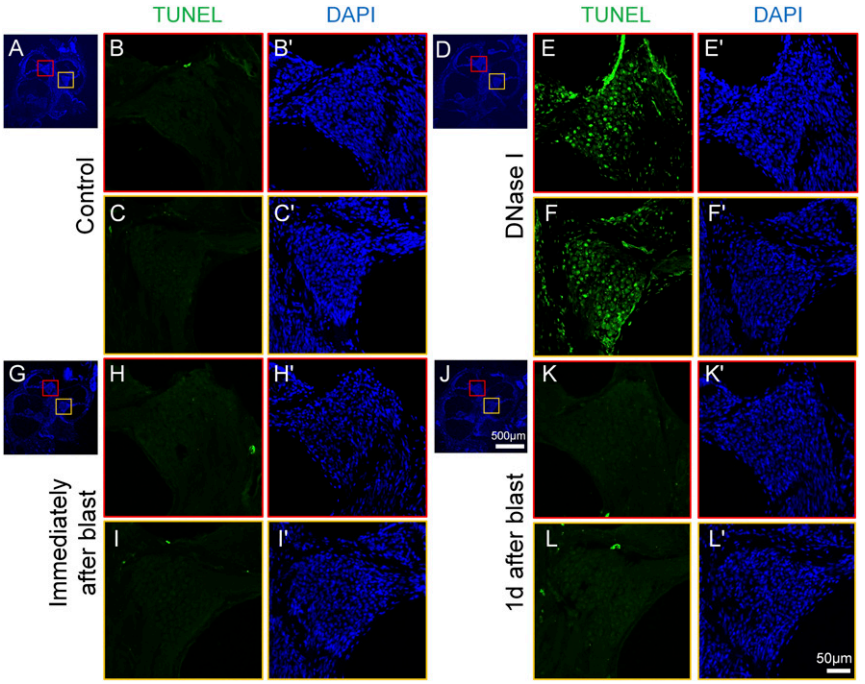

Fig. S2. TUNEL assay demonstrates no DNA trauma within spiral ganglion neurons after the blast. (*A*, *D*, *G*, and *J*) Cochlear midmodiolar cross-sections highlighting the regions of the spiral ganglion expanded in the close-ups (apical turn: red; basal turn: yellow). (*A–C*) Unexposed control mouse. (*D–F*) Positive control treated with DNase I. (*G–I*) Immediately after the blast. (*J–L*) One day after the blast.

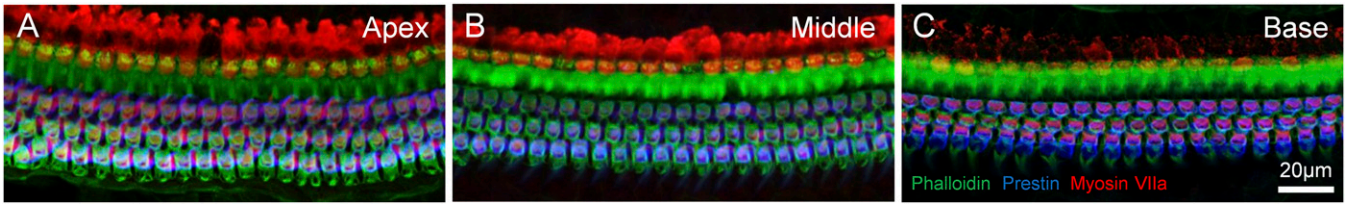

Fig. S3. Immunolabeled images of the cochlear epithelium from a representative *Tecta*$^{C1509G/C1509G}$ mouse. (*A–C*) Immunolabeling was done to visualize all hair cells (myosin VIIa) and OHCs (Prestin). Seven days after blast exposure, there was no loss of hair cells in the apical, middle, or basal cochlear regions (n = 5 mice).

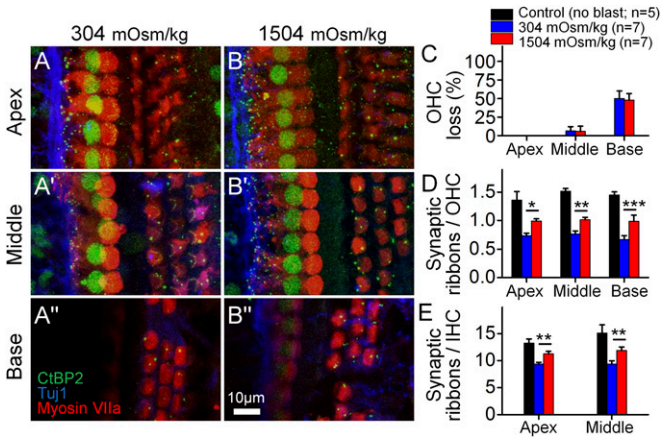

Fig. S4. Osmotic stabilization of endolymphatic hydrops with hypertonic saline partially rescues cochlear synaptopathy after blast exposure. (*A* and *B*) The cochlear epithelium from representative mice 7 d after blast exposure. Mice had either normotonic or hypertonic saline applied within the middle ear 30 min after the blast. Immunolabeling was done to visualize synaptic ribbons in hair cells (CtBP2), hair cells (myosin VIIa), and auditory neurons (Tuj1). (*C–E*) Quantification of OHC loss and synaptic ribbons per OHC and IHC. Hypertonic saline reduced the loss of synaptic ribbons but did not affect the degree of OHC loss. $*P < 0.05$, $**P < 0.01$, $***P < 0.001$.

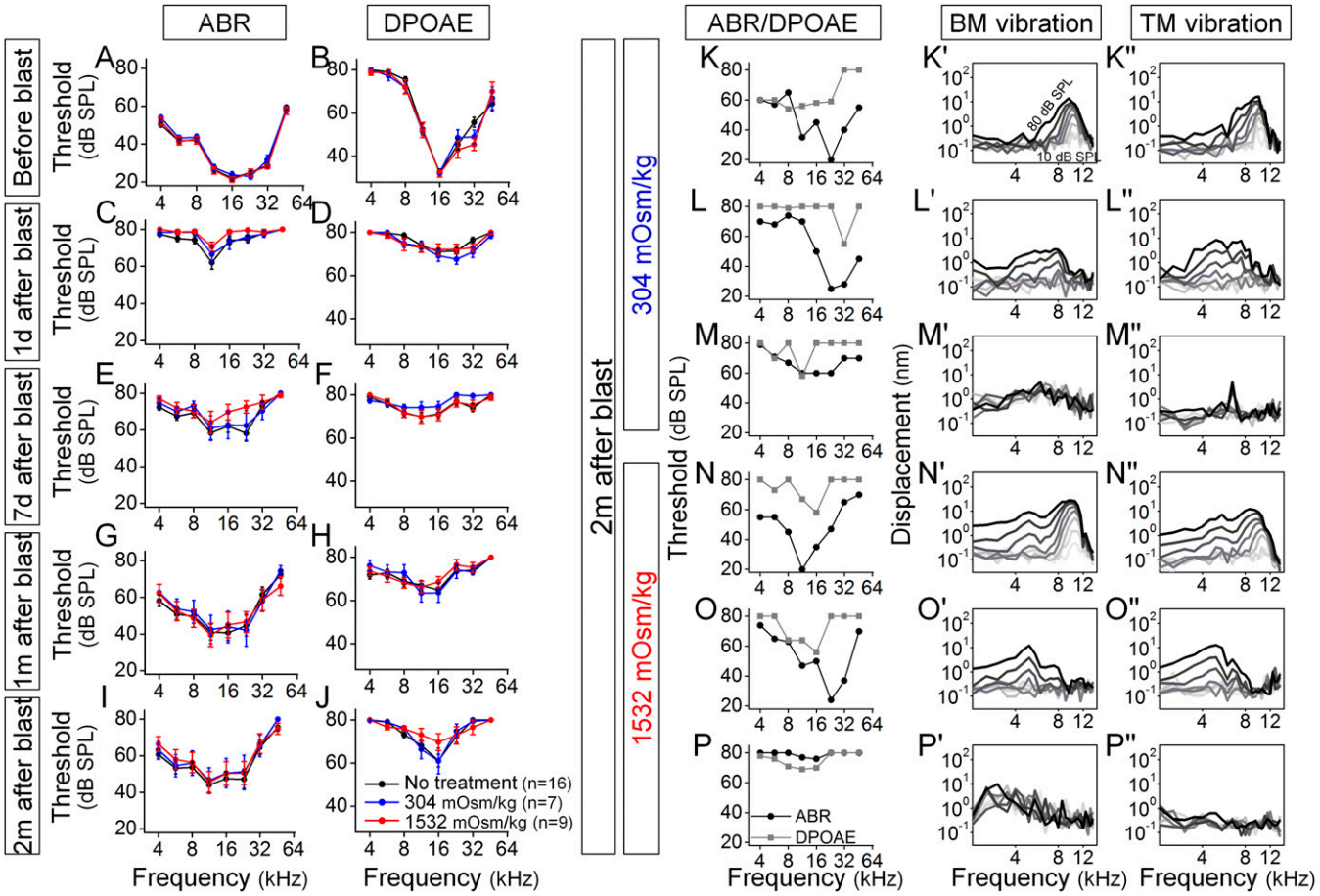

Fig. S5. Auditory thresholds and vibratory responses after blast exposure followed by osmotic challenge. ABR (*A*, *C*, *E*, *G*, and *I*) and DPOAE (*B*, *D*, *F*, *H*, and *J*) thresholds before the blast, 1 d, 7 d, 1 mo, and 2 mo after blast exposure. Either normotonic (304 mOsm/kg) or hypertonic (1,532 mOsm/kg) artificial perilymph was applied into the middle ear beginning 30 min after blast exposure and continuing for another 5.5 h. There were no differences in threshold recovery between the hypertonic, normotonic, and untreated cohorts 2 mo after the blast (ABR: $P = 0.28$; DPOAE: $P = 0.66$). (*K*–*P*) Representative ABR, DPOAE thresholds, BM, and TM vibratory responses 2 mo after blast exposure. Representative results from three mice per each cohort are shown to demonstrate the wide range of variability. Some mice demonstrated large compressive nonlinearity consistent with normal cochlear amplification (*K* and *N*) even though the peak amplitudes were lower than unexposed mice, suggesting the presence of middle ear trauma that caused conductive hearing loss. Some mice had purely passive vibratory responses, indicating no cochlear amplification (*L* and *O*). Other mice had no vibratory responses at all, suggesting there was substantial conductive hearing loss (*M* and *P*).

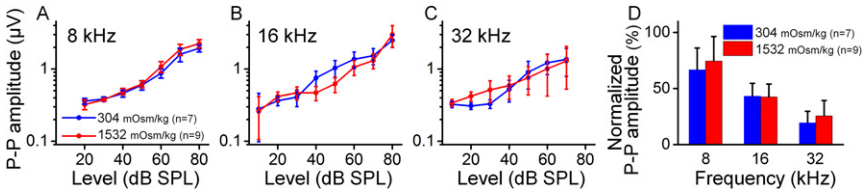

Fig. S6. ABR wave I peak-to-peak amplitudes after blast exposure followed by osmotic challenge. Raw ABR wave I amplitudes over the range of stimulus intensities that were delivered at 8 kHz (*A*), at 16 kHz (*B*), at 32 kHz (*C*). (*D*) The ABR wave I amplitude in response to 70-dB SPL stimuli at 8, 16, and 32 kHz 2 mo after blast exposure was normalized to the amplitude of wave I measured before the blast exposure. This was done in an effort to account for differences between individual mice. There were no differences between the hypertonic and normotonic treated cohorts 2 mo after the blast at any frequency.

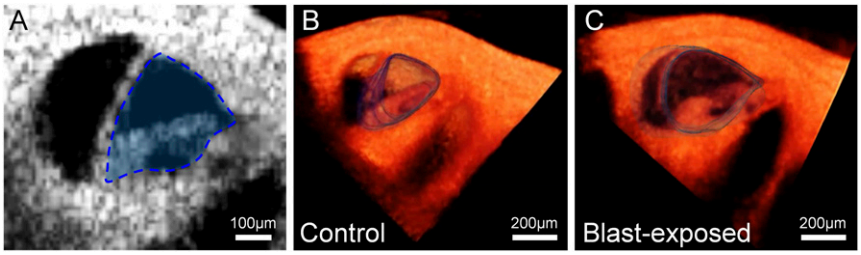

Fig. S7. Method for calculating endolymph volume. (*A*) A single cross-section of the apical turn of the mouse cochlea. The blue highlights the region of scala media manually segmented out to calculate endolymph volume. (*B* and C) Three-dimensional volume-rendered OCT images. Examples of segmented cochlear volumes from a control mouse (*B*) and a mouse 3 h after blast exposure (*C*). The length of the BM within the volume was 150 μm.

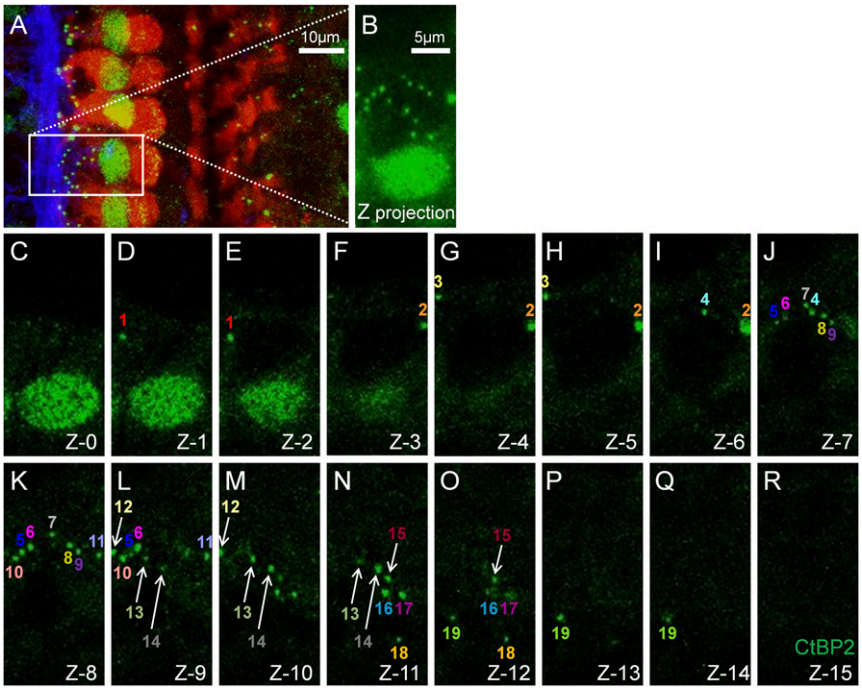

Fig. S8. Method for counting synaptic densities. (*A*) A representative summed voxel projection of a mouse cochlea immunolabeled with CtBP2, myosin VIIa, and Tuj1, like that shown in Figs. 2, 5, and 6 and Fig. S4. The white box highlights the area under one IHC. (*B*) The summed voxel projection of the CtBP2 channel. (*C*–*R*) Sequential *z*-stack images that make up the summed voxel projection. The images start near the top (*C*) and go toward the bottom (*R*) of the epithelium. The images were collected every 0.981 μm. A scan range of 14.716 μm is shown here, which covers the entire thickness of the region around the IHC. Synaptic densities were only counted if they showed up on at least two sequential images. Each number in the figure identifies one synaptic density. In this example, there were 19 CtBP2-labeled synaptic densities for this IHC.

Table S1. Statistical test *P* values

	Group							
Figure	1	2	3	4	5	6	*P* value	Test
Fig. 1*K*	Control 1 h	Control 2 h	Control 3 h	—	—	—	0.28	ANOVA
Fig. 1*K*	Postmortem 1 h	Postmortem 2 h	—	—	—	—	0.013	PTT
Fig. 1*K*	Postmortem 1 h	Postmortem 3 h	—	—	—	—	0.002	PTT
Fig. 1*K*	Blast 1 h	Blast 2 h	—	—	—	—	<0.001	PTT
Fig. 1*K*	Blast 1 h	Blast 3 h	—	—	—	—	<0.001	PTT
Fig. 1*K*	Control 1 h	Blast 1 d	—	—	—	—	0.303	UTT
Fig. 2*B*	TUNEL (+) OHC (middle)	7d OHC loss (middle)	—	—	—	—	0.743	UTT
Fig. 2*B*	TUNEL (+) OHC (base)	7d OHC loss (base)	—	—	—	—	0.629	UTT
Fig. 2*Q*	Control OHC (apex)	Blast OHC (apex)	—	—	—	—	0.009	UTT
Fig. 2*Q*	Control OHC (middle)	Blast OHC (middle)	—	—	—	—	<0.001	UTT
Fig. 2*Q*	Control OHC (base)	Blast OHC (base)	—	—	—	—	0.009	UTT
Fig. 2*R*	Control IHC (apex)	Blast IHC (apex)	—	—	—	—	0.004	UTT
Fig. 2*R*	Control IHC (middle)	Blast IHC (middle)	—	—	—	—	<0.001	UTT
Fig. 3*C*	Control SM	Control SV	—	—	—	—	0.039	PTT
Fig. 3*C*	Blast SM	Blast SV	—	—	—	—	0.015	PTT
Fig. 3*C*	Control SM	Blast SM	—	—	—	—	0.976	PTT
Fig. 3*C*	Control SV	Blast SV	—	—	—	—	0.632	PTT
Fig. 4*C*	Tecta control 1 h	Tecta control 2 h	Tecta control 3 h	Tecta blast 1 h	Tecta blast 2 h	Tecta blast 3 h	0.80	ANOVA
Figs. 1*K* and 4*C*	CBA control 1 h	Tecta control 1 h	—	—	—	—	0.002	UTT
Figs. 1*K* and 4*G*	CBA control 1 h	*Tyr*-DT-A control 1 h	—	—	—	—	0.007	UTT
Fig. 4*G*	*Tyr*-DT-A control 1 h	*Tyr*-DT-A control 2 h	*Tyr*-DT-A control 3 h	*Tyr*-DT-A blast 1h	*Tyr*-DT-A blast 2 h	*Tyr*-DT-A blast 3 h	0.76	ANOVA
Fig. 4*J*	CBA furosemide 1 h	CBA furosemide 2 h	CBA furosemide 3 h	—	—	—	0.96	ANOVA
Fig. 4*J*	Blast 1 h	Blast + furosemide 1 h	—	—	—	—	<0.001	UTT
Fig. 4*J*	Blast 2 h	Blast + furosemide 2 h	—	—	—	—	<0.001	UTT
Fig. 4*J*	Blast 3 h	Blast + furosemide 3 h	—	—	—	—	<0.001	UTT
Fig. 5*L*	Hypertonic 3 h	Hypertonic 3.5 h	—	—	—	—	<0.001	PTT
Fig. 5*L*	Normotonic 3 h	Normotonic 3.5 h	—	—	—	—	0.442	PTT
Fig. 5*P*	Untreated OHC (apex)	Normotonic OHC (apex)	Hypertonic OHC (apex)	—	—	—	1.0	ANOVA
Fig. 5*P*	Untreated OHC (middle)	Normotonic OHC (middle)	Hypertonic OHC (middle)	—	—	—	0.769	ANOVA
Fig. 5*P*	Untreated OHC (base)	Normotonic OHC (base)	Hypertonic OHC (base)	—	—	—	0.666	ANOVA
Fig. 5*Q*	Control OHC CtBP2 (apex)	Blast OHC CtBP2 (apex)	—	—	—	—	<0.001	UTT
Fig. 5*Q*	Control OHC CtBP2 (middle)	Blast OHC CtBP2 (middle)	—	—	—	—	<0.001	UTT
Fig. 5*Q*	Control OHC CtBP2 (base)	Blast OHC CtBP2 (base)	—	—	—	—	<0.001	UTT
Fig. 5*Q*	Control OHC CtBP2 (apex)	Blast + normotonic OHC CtBP2 (apex)	—	—	—	—	0.004	UTT
Fig. 5*Q*	Control OHC CtBP2 (middle)	Blast + normotonic OHC CtBP2 (middle)	—	—	—	—	<0.001	UTT
Fig. 5*Q*	Control OHC CtBP2 (base)	Blast + normotonic OHC CtBP2 (base)	—	—	—	—	<0.001	UTT
Fig. 5*Q*	Blast OHC CtBP2 (apex)	Blast + hypertonic OHC CtBP2 (apex)	—	—	—	—	<0.001	UTT
Fig. 5*Q*	Blast OHC CtBP2 (middle)	Blast + hypertonic OHC CtBP2 (middle)	—	—	—	—	<0.001	UTT

Table S1. Cont.

Figure	Group 1	2	3	4	5	6	*P* value	Test
Fig. 5*Q*	Blast OHC CtBP2 (base)	Blast + hypertonic OHC CtBP2 (base)	—	—	—	—	<0.001	UTT
Fig. 5*Q*	Blast + normotonic OHC CtBP2 (apex)	Blast + hypertonic OHC CtBP2 (apex)	—	—	—	—	0.002	UTT
Fig. 5*Q*	Blast + normotonic OHC CtBP2 (middle)	Blast + hypertonic OHC CtBP2 (middle)	—	—	—	—	<0.001	UTT
Fig. 5*Q*	Blast + normotonic OHC CtBP2 (base)	Blast + hypertonic OHC CtBP2 (base)	—	—	—	—	0.004	UTT
Fig. 5*R*	Control IHC CtBP2 (apex)	Blast IHC CtBP2 (apex)	—	—	—	—	<0.001	UTT
Fig. 5*R*	Control IHC CtBP2 (middle)	Blast IHC CtBP2 (middle)	—	—	—	—	<0.001	UTT
Fig. 5*R*	Control IHC CtBP2 (apex)	Blast + normotonic IHC CtBP2 (apex)	—	—	—	—	<0.001	UTT
Fig. 5*R*	Control IHC CtBP2 (middle)	Blast + normotonic IHC CtBP2 (middle)	—	—	—	—	<0.001	UTT
Fig. 5*R*	Blast IHC CtBP2 (apex)	Blast + hypertonic IHC CtBP2 (apex)	—	—	—	—	<0.001	UTT
Fig. 5*R*	Blast IHC CtBP2 (middle)	Blast + hypertonic IHC CtBP2 (middle)	—	—	—	—	<0.001	UTT
Fig. 5*R*	Blast + normotonic IHC CtBP2 (apex)	Blast + hypertonic IHC CtBP2 (apex)	—	—	—	—	<0.001	UTT
Fig. 5*R*	Blast + normotonic IHC CtBP2 (middle)	Blast + hypertonic IHC CtBP2 (middle)	—	—	—	—	0.002	UTT
Fig. 6*K*	Control OHC CtBP2 (apex)	Hypotonic OHC CtBP2 (apex)	—	—	—	—	0.009	UTT
Fig. 6*K*	Control OHC CtBP2 (middle)	Hypotonic OHC CtBP2 (middle)	—	—	—	—	<0.001	UTT
Fig. 6*K*	Control OHC CtBP2 (base)	Hypotonic OHC CtBP2 (base)	—	—	—	—	<0.001	UTT
Fig. 6*L*	Control IHC CtBP2 (apex)	Hypotonic IHC CtBP2 (apex)	—	—	—	—	0.01	UTT
Fig. 6*L*	Control IHC CtBP2 (middle)	Hypotonic IHC CtBP2 (middle)	—	—	—	—	0.006	UTT
Fig. 6*K*	Blast 6h OHC CtBP2	Blast 7d OHC CtBP2	Blast 2M OHC CtBP2	Hypotonic OHC CtBP2	—	—	0.10	ANOVA
Fig. 6*L*	Blast 6h IHC CtBP2	Blast 7d IHC CtBP2	Blast 2M IHC CtBP2	Hypotonic IHC CtBP2	—	—	0.15	ANOVA
Fig. 6*P*	Control IHC CtBP2	Normotonic IHC CtBP2	Normotonic IHC Homer	—	—	—	0.97	ANOVA
Fig. 6*P*	Normotonic IHC CtBP2	Hypotonic IHC CtBP2	—	—	—	—	0.01	UTT
Fig. 6*P*	Normotonic IHC Homer	Hypotonic IHC Homer	—	—	—	—	0.02	UTT
Fig. 6*P*	Normotonic IHC CtBP2	Hypotonic +CNQX IHC CtBP2	—	—	—	—	0.29	UTT
Fig. 6*P*	Normotonic IHC Homer	Hypotonic +CNQX IHC Homer	—	—	—	—	0.70	UTT
Fig. 6*Q*	Normotonic colocalization	Hypotonic colocalization	—	—	—	—	0.04	UTT
Fig. 6*Q*	Normotonic colocalization	Hypotonic +CNQX colocalization	—	—	—	—	0.72	UTT

PTT, Student's two-tailed paired *t* test; UTT, Student's two-tailed unpaired *t* test.

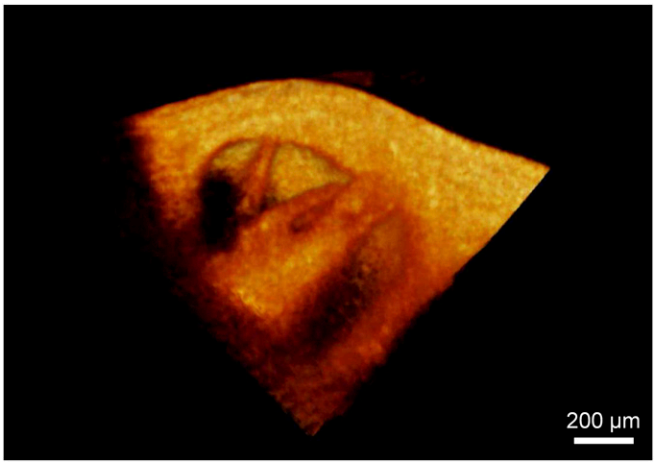

Movie S1. Three-dimensional volume of the apical turn of the mouse cochlea. This is the volume from which we calculated the endolymph volume.

Movie S1

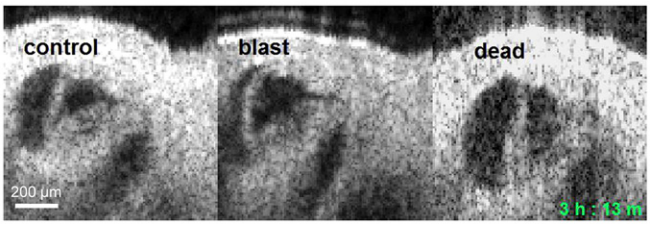

Movie S2. Time-lapse series of a normal control mouse (*Left*), a blast-exposed mouse (*Center*), and a dead mouse (*Right*). The time after induction of anesthesia is given in the corner.

Movie S2

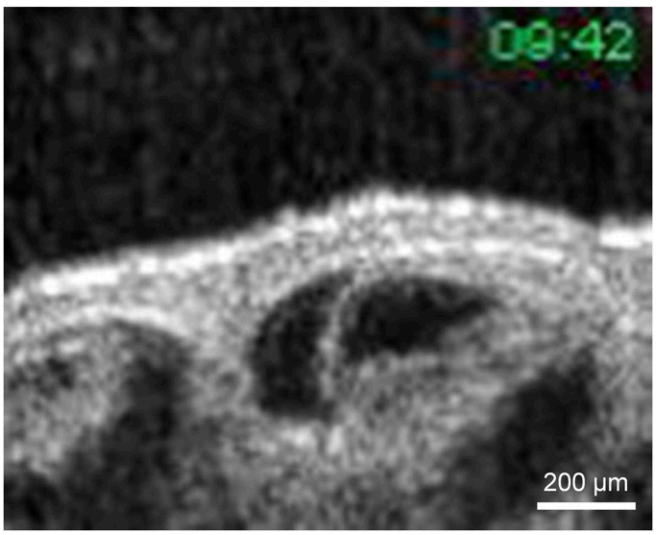

Movie S3. Time-lapse series of a blast-exposed mouse. The time after blast exposure is given in the corner.

Movie S3

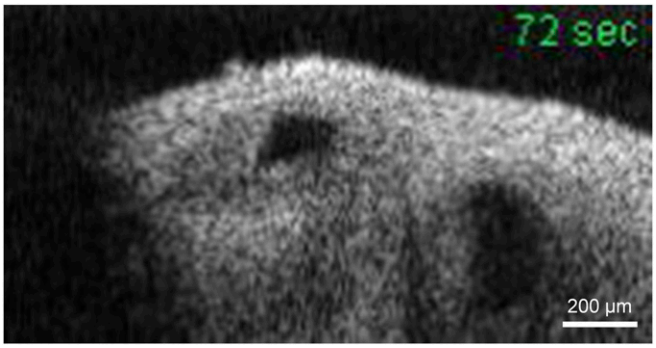

Movie S4. Perilymphatic perfusion of gold nanoparticles in a control mouse. The time after perfusion started is given in the corner.

Movie S4

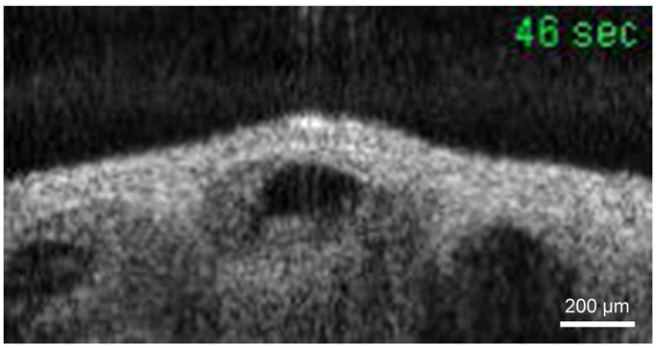

Movie S5. Perilymphatic perfusion of gold nanoparticles in a mouse 3 h after blast exposure. The time after perfusion started is given in the corner.

Movie S5